Following Reaction Pathways Using a Damped Classical Trajectory Algorithm

H. P. Hratchian and H. B. Schlegel*

Department of Chemistry and Institute for Scientific Computing, Wayne State University, Detroit, Michigan 48202-3489

Received: June 5, 2001; In Final Form: October 17, 2001

The study of reaction pathways is imperative to the investigation of potential energy surfaces. The intrinsic reaction coordinate is defined as the steepest descent path in mass weighted coordinates that connects the transition state to reactants and products. Various methods are available for following the intrinsic reaction coordinate. A potential energy surface may also be studied using classical trajectory calculations, and a dynamic reaction path method can be used to connect the transition state to reactants and products. We have modified a classical trajectory integration method such that the dynamic reaction pathway more closely resembles the intrinsic reaction coordinate. Specifically, a damped velocity Verlet algorithm incorporating a controlled time step is used. The efficiency of the present algorithm is on the same order as our earlier methods for relatively small systems and shows increasing efficiency as the large molecule limit is approached.

I. Introduction

The theoretical study of a chemical reaction typically first requires finding relevant stationary points on the potential energy surface (PES) and then confirming that a suitable pathway connects those points. Methods for finding equilibrium geometries and transition state (TS) structures have been reviewed extensively.[1−8] After a TS has been located, one may verify that it connects the desired reactants and products by determining the minimum energy pathway (MEP). Typically, this task is achieved by an intrinsic reaction coordinate (IRC) analysis. The IRC is defined as the steepest descent path from the TS in mass weighted Cartesian coordinates.[9]

The steepest descent path can be obtained by integrating the differential equation

$$\frac{d\mathbf{x}(s)}{ds} = -\frac{\mathbf{g}(\mathbf{x})}{|\mathbf{g}(\mathbf{x})|} \tag{1}$$

where **x** is the path, *s* is the arc length along the path, and **g** is the gradient of the PES. Because eq 1 corresponds to a stiff differential equation, some care is needed in integrating it. Numerous methods for following the IRC have been suggested in the literature (for an overview, see ref 10).[4,7,10−22] IRC following algorithms can be divided into two categories: implicit and explicit methods. Implicit methods require derivative information at the current point and the point at the end of each step; explicit methods depend only upon information at the current position. Computationally, explicit procedures are simpler to implement. Explicit algorithms include Euler's method, the Ishida-Morokuma-Komornicki (stabilized Euler) method,[12,13] Runge−Kutta and predictor-corrector methods,[14,15] the local quadratic approximation (LQA),[16,17] and the Sun−Ruedenberg modification of LQA, etc.[18] Some of these methods require only gradient information and are limited to rather small step sizes, while others also use the Hessian. Methods that use second derivatives are more costly, but gain additional stability and allow for larger step sizes.

Implicit methods for differential equations are more difficult to implement because the gradient at the point at the end of a step must be obtained iteratively or by approximation.[23] Though more costly, implicit algorithms are more stable than explicit methods and allow for good performance with larger step sizes. Implicit methods for IRC analysis include the Müller−Brown (implicit Euler) method[19] and the second-order method of Gonzalez and Schlegel (implicit trapezoid)[20,21] and higher order methods by the same authors.[22]

Alternatively, the PES can be explored using classical trajectory calculations.[8,24−26] The differential equations describing the classical equations of motion are much easier to solve by numerical methods. Until recently, classical trajectory calculations relied heavily upon accurate global knowledge of the PES under study.[8,24−26] Now it is possible to carry out this type of calculation directly from electronic structure calculations without first needing to fit a global PES.[27]

The dynamic reaction path (DRP) method[28−30] uses trajectory calculations to follow the IRC approximately. If a trajectory were begun at the TS heading in the direction of the transition vector and all kinetic energy were continuously removed from the system, the DRP would be identical to the IRC. Maluendas and Dupuis have described a DRP method that closely follows the IRC path without requiring that the kinetic energy be zero.[29] Their method is based on the dynamic reaction coordinate (DRC) as defined by Stewart et al.[30] and uses the Gear predictor-corrector method (GPC) for integrating the differential equations.[31]

In their study, Maluendas and Dupuis compared their GPC and DRC approaches to time-independent MEP calculations. Specifically, they tested the efficiencies of GPC and DRC by comparing the number of gradient calculations needed to map out the reaction pathway to that of the IRC approach of Schmidt et al.[12] The present paper outlines a similar method for approximating the IRC pathway using classical trajectories. The velocity Verlet algorithm is used to integrate the trajectory, and the velocity is adjusted after every step so that the magnitude remains constant and nonzero throughout the calculation. We employ a time variation scheme at every step along the path to

* To whom correspondence should be addressed. E-mail: hbs@chem.wayne.edu.

10.1021/jp012125b CCC: $22.00
Published on Web 12/08/2001

make adjustments for future time steps based on estimated errors in the path. Maluendas and Dupuis also employ a time variation scheme; however, their time variation mechanism is used in conjunction with kinetic energy resetting when oscillations in the path or deviations from the MEP are recognized. The continuous damping and time step adjustment used in the present method are particularly advantageous for larger systems. To show the utility of this method, we have calculated pathways for a number of reactions and compared them to IRC paths integrated with the second-order method of Gonzales and Schlegel (GS−IRC).[20,21] The efficiency and stability of the GS−IRC method has been demonstrated previously.[20]

II. Method

The present method adapts the direct classical trajectory code in the Gaussian [32] series of programs to provide a reaction path following algorithm that is more suitable for large molecules than the GS−IRC procedure. The velocity Verlet algorithm is an efficient scheme for propagation of a trajectory and lends itself to easy adjustment of step size. By controlling the magnitude of the velocity vector and the time step size at every step along the path, it is possible to make the damped velocity Verlet (DVV) trajectory approach the IRC path within a chosen tolerance. Each DVV step is composed of three parts:

1. Position and velocity vectors are propagated to the next point along the DVV pathway using the velocity Verlet method;
2. The magnitude of the velocity is damped; and
3. The deviation of the DVV path from the IRC path is estimated as a function of the time step and the time step is then updated.

Velocity Verlet, a gradient dependent method, determines the position, **x**, and velocity, **v**, at step *i* according to

$$\mathbf{x}_i = \mathbf{x}_{i-1} + \mathbf{v}_{i-1}\,\Delta t_i + \frac{1}{2}\,\mathbf{a}_{i-1}\,\Delta t_i^2$$

$$\mathbf{v}_i = \mathbf{v}_{i-1} + \frac{1}{2}\,(\mathbf{a}_{i-1} + \mathbf{a}_i)\,\Delta t_i \qquad (2)$$

The acceleration, **a**, is the product of the inverse of the diagonal matrix of atomic masses, **m**, and the force where the force is defined as the negative of the energy gradient

$$\mathbf{a} = -\mathbf{m}^{-1}\,\mathbf{g}(\mathbf{x}) \qquad (3)$$

After each DVV step, the velocity is multiplied by a damping factor such that the magnitude of the velocity vector is set equal to a constant υ_0

$$|\mathbf{v}_i| = \upsilon_0 \qquad (4)$$

The initial position vector is the transition structure and the direction of the initial velocity vector is taken as the transition vector; the path integration is carried out in both the forward and reverse directions.

To ensure that the damped trajectory stays close to the IRC, we control the integration error by adjusting the time step. The error in a velocity Verlet integration scheme scales as Δt^3. If the desired error is Δ_0, an appropriate time step, Δt_{i+1}, for the next step can be determined from the current time step, Δt_i, and the estimated error for the current step, Δ_i

$$\Delta t_{i+1} = \Delta t_i \left|\frac{\Delta_0}{\Delta_i}\right|^{1/3} \qquad (5)$$

The error tolerance Δ_0 is provided by the user. Equation 5 offers the ability to increase the time step when the estimated error is smaller than the tolerance and to decrease the time step when the error exceeds the allowed tolerance. In the present study, Δ_0 is set to 0.003 bohr, and the time step is constrained such that 0.025 fs $\leq \Delta t \leq$ 3.000 fs.

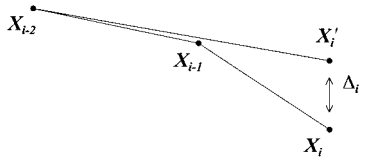

Figure 1. Estimation of the error in the propagation of the DVV path (see text).

The estimated error for the current step is taken as the larger of the magnitude or the largest component of the displacement vector between a point, $\mathbf{x}_i'$, and the current point, $\mathbf{x}_i$. As shown in Figure 1, the point $\mathbf{x}_i'$ is obtained by propagating from $\mathbf{x}_{i-2}$ and $\mathbf{v}_{i-2}$ with a time step equal to the sum of Δt_i and Δt_{i-1}

$$\mathbf{x}_i' = \mathbf{x}_{i-2} + \mathbf{v}_{i-2}\,(\Delta t_{i-1} + \Delta t_i) + \frac{1}{2}\,\mathbf{a}_{i-2}\,(\Delta t_{i-1} + \Delta t_i)^2 \qquad (6)$$

This provides a simple means of estimating the error and adjusting the time step while not demanding additional gradient calculations.

III. Applications

The present algorithm has been implemented in the development version of Gaussian[32] and has been tested on a number of reactions chosen to provide a variety of reaction types. For reference, results are compared to the GS−IRC implicit method,[20,21] which has been found to be efficient and stable in numerous previous applications. GS−IRC pathways were calculated using the default step size of 0.1 amu$^{1/2}$ bohr (larger step sizes may also yield suitable paths). The GS−IRC algorithm requires an optimization for each step taken; the number of optimization steps needed to correct each IRC step may increase with the number of atoms in the system being studied.

For large systems, the electronic structure calculations are done by direct methods and the computational time is proportional to the number of Fock matrix evaluations. In turn, the number of Fock matrix evaluations needed to converge a typical SCF calculation depends on the step size taken from the previous point rather than the size of the system. Thus, in anticipation of applications to larger systems, the number of Fock matrix evaluations is used to compare the efficiency of the present method to the GS−IRC approach (see Table 1).

A. $CH_4 + F \rightarrow CH_3 + HF$. Abstraction reactions are important processes in combustion. One example of this reaction type is $CH_4 + F \rightarrow CH_3 + HF$. Calculations were preformed at the HF/3-21G level of theory. DVV reaction pathways were computed with υ_0 set to 0.04, 0.08, and 0.20 bohr/fs. Figure 2 shows the relationship between the C—H and F—H bond lengths from calculations using each of the given step sizes and the pathway predicted by the GS−IRC method. This plot displays the relative stability of the DVV algorithm even when large velocity values are used. The data in Table 1 indicate that the DVV method is much less efficient in this case than the GS−IRC algorithm when υ_0 is equal to 0.04 bohr/fs. However, the difference between the GS−IRC and the DVV calculations when 0.08 bohr/fs is used for υ_0 is relatively small indicating that the cost for the DVV calculation for this system is roughly the same as for the GS−IRC approach.

TABLE 1: Comparison of the Number of Fock Evaluations for DVV and IRC Calculations

reaction	Fock evaluations for DVV ($\upsilon_0 = 0.04$ au/fs)	Fock evaluations for DVV ($\upsilon_0 = 0.08$ au/fs)	Fock evaluations for IRC[a]
$CH_4 + F \rightarrow CH_3 + HF$	1276	817	716
$CH_2OH \rightarrow CH_3O$	1236	861	1352
Diels − Alder	2142	1081	1352
$CH_3CH_2F \rightarrow CH_2CH_2 + HF$	1439	1453	4281
Ene	2134	2518	7406
$[Ir(CO)_2I_3(CH_3)]^- \rightarrow Ir(CO)I_3(COCH_3)]^-$	1078		9579

[a] GS−IRC calculations were run with a step size equal to 0.1 $amu^{1/2}$ bohr.

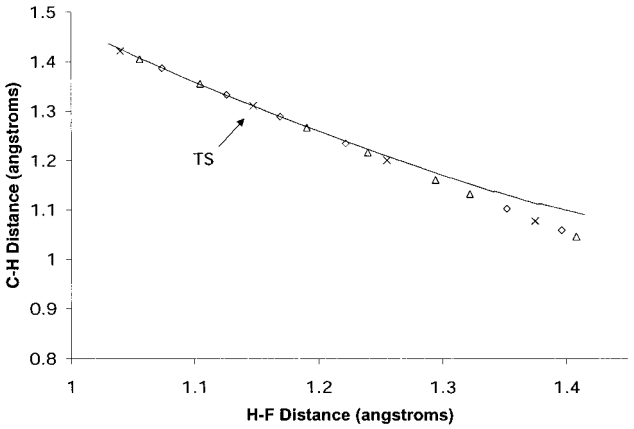

Figure 2. Reaction path following for $CH_4 + F \rightarrow CH_3 + HF$ [DVV paths with υ_0 equal to 0.04 (◇), 0.08 (△), and 0.20 (×) bohr/fs, and GS−IRC path (solid line) − every third point shown; overlapping points have been removed for clarity].

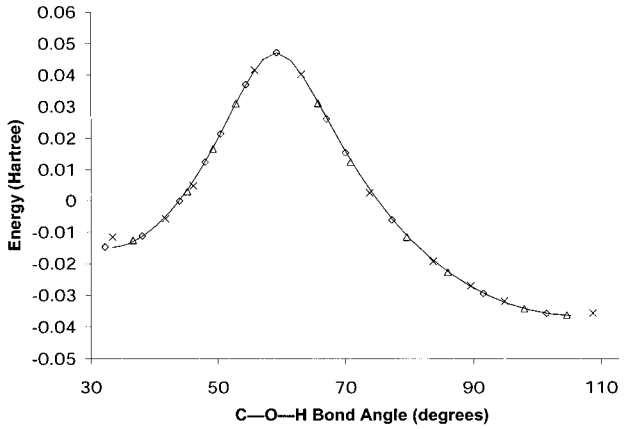

Figure 3. Reaction path following for $CH_2OH \rightarrow CH_3O$ [DVV paths with υ_0 equal to 0.04 (◇), 0.08 (△), and 0.20 (×) bohr/fs, and GS−IRC path (solid line)].

B. $CH_2OH \rightarrow CH_3O$. This reaction, a 1, 2 hydrogen shift, serves as a good model for 1, *n* group shift reactions. Calculations were preformed at the AM1 level of theory. The relationship between the C—O—H bond angle and energy is given as Figure 3. Again, the current algorithm proves to be very stable for all values of υ_0 considered. As seen in Table 1, our method requires 1236 and 861 Fock matrix evaluations to follow the complete reaction pathway when υ_0 is equal to 0.04 and 0.08 bohr/fs, respectively. The GS−IRC calculation requires 1352 Fock matrix evaluations.

C. Diels−Alder Reaction. The reaction of butadiene with ethylene is the prototypical example of the Diels−Alder reaction and proceeds through a pericyclic TS. A reaction profile is given as Figure 4 based on results from DVV calculations at the AM1 level of theory with υ_0 set to 0.04, 0.08, and 0.20 bohr/fs. As

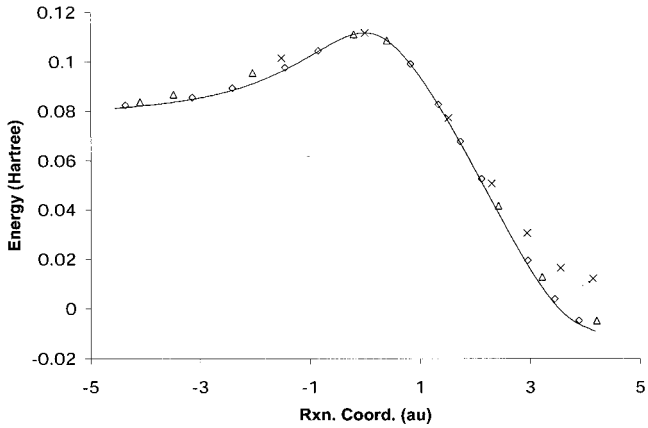

Figure 4. Reaction path following for the Diels−Alder reaction [DVV paths with υ_0 equal to 0.04 (◇), 0.08 (△), and 0.20 (×) bohr/fs, and GS−IRC path (solid line)].

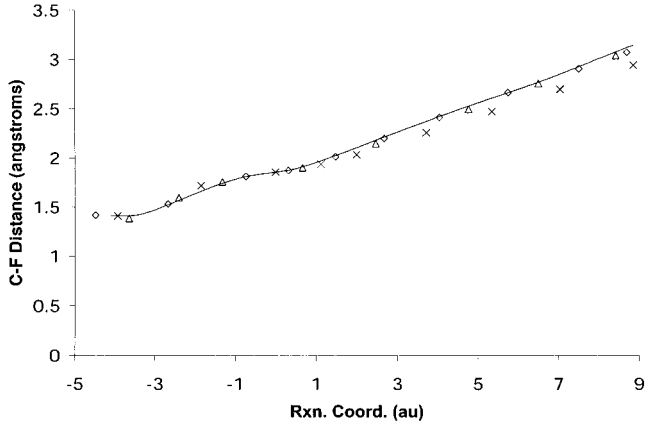

Figure 5. Reaction path following for $CH_3CH_2F \rightarrow CH_2CH_2 + HF$ [DVV paths with υ_0 equal to 0.04 (◇), 0.08 (△), and 0.20 (×) bohr/fs, and GS−IRC path (solid line)].

before, the results of a GS−IRC calculation have been included to provide comparison. The DVV reaction path mimics the GS−IRC pathway very well when υ_0 is relatively small, while deviations begin to appear when υ_0 is equal to 0.20 bohr/fs. The present method requires 2142 and 1081 Fock matrix evaluations to follow the complete reaction pathway when υ_0 is 0.04 and 0.08 bohr/fs, respectively, while the GS−IRC algorithm requires 1352 Fock matrix evaluations.

D. $CH_3CH_2F \rightarrow CH_2CH_2 + HF$. This reaction is a standard example of four-center elimination, and has been studied by Kato and Morokuma.[34] Ab initio calculations have been carried out at the HF/3-21G level of theory. Calculations employed values for υ_0 of 0.04, 0.08, and 0.20 bohr/fs. Figure 5 is a plot of C—F bond length against reaction coordinate, and Figure 6 shows the relationship between the H—F bond length and potential energy. Figure 5 suggests very good agreement with

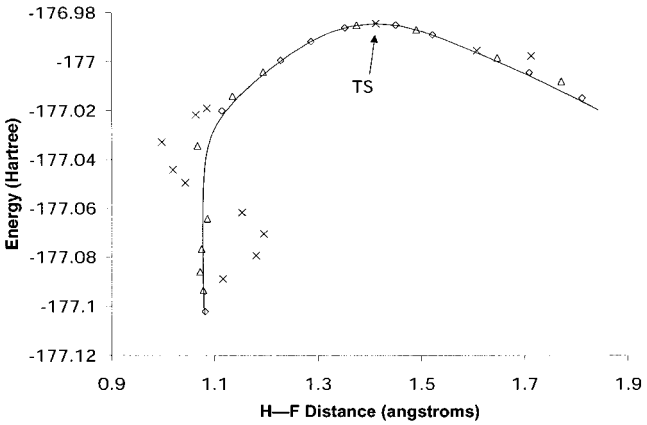

Figure 6. Reaction path following for $CH_3CH_2F \rightarrow CH_2CH_2 + HF$ [DVV paths with υ_0 equal to 0.04 0.04 (◇), 0.08 (△), and 0.20 (×) bohr/fs, and GS−IRC path (solid line)].

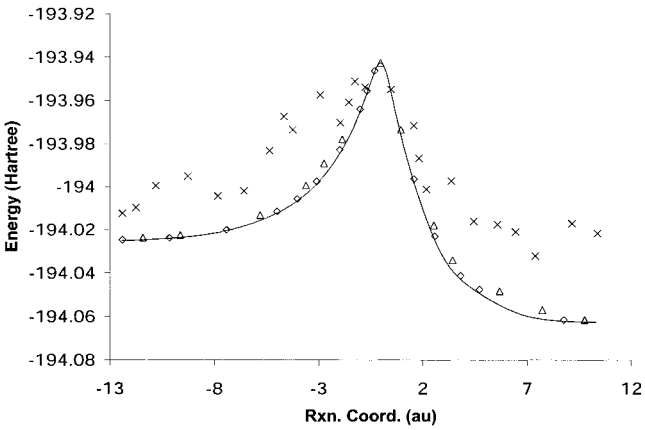

Figure 7. Reaction path following for the ene reaction [DVV paths with υ_0 equal to 0.04 (◇), 0.08 (△), and 0.20 (×) bohr/fs, and GS−IRC path (solid line)].

the GS−IRC pathway for all three υ_0 values shown. Figure 6 shows very good agreement between the DVV and IRC paths when υ_0 is equal to 0.04 and 0.08 bohr/fs. However, when $\upsilon_0 = 0.20$ bohr/fs the DVV path deviates greatly from the IRC path resulting from vibration of the H—F bond. As noted in Table 1, the GS−IRC method requires 4281 Fock matrix evaluations to explore the MEP; the number of gradient evaluations required by the GS−IRC method is also about 3 times greater than for the DVV approach. The reaction path is mapped out using the DVV algorithm in 1439 Fock evaluations for $\upsilon_0 = 0.04$ bohr/fs and in 1453 Fock evaluations for $\upsilon_0 = 0.08$ bohr/fs. As seen in Figure 6, the pathway for $\upsilon_0 = 0.08$ bohr/fs shows very subtle oscillations when the H—F bond distance is short. This deviation in the path is corrected by the time step variation algorithm resulting in a slower progression along the reaction path. The average time step value when υ_0 is 0.04 bohr/fs is 1.098 fs, whereas Δt is 0.543 fs on average when $\upsilon_0 = 0.08$ bohr/fs. This in turn leads to a slight increase in the number of Fock matrix evaluations for the $\upsilon_0 = 0.08$ bohr/fs case. Nevertheless, both DVV calculations are much more efficient than the GS−IRC approach.

E. Ene reaction: $CH_2{=}CH{-}CH_2{-}CH_2{-}CH_3 \rightarrow CH_3{-}CH{=}CH_2 + CH_2{=}CH_2$. The ene reaction proceeds through a six-member ring TS where two bonds are broken and two others are formed. Previous studies have used this system because of the difficulty associated with finding its transition state.[35] This example displays the strength of the DVV method: increasing efficiency with increasing system size and complexity. Calculations have been carried out at the HF/3-21G level of theory, and the reaction path profile is shown as Figure 7. The present method duplicates the GS−IRC pathway very well when υ_0 is 0.04 and 0.08 bohr/fs, but when υ_0 is equal to 0.20 bohr/fs, the DVV path displays significant oscillations in both the reactant and product channels. For $\upsilon_0 = 0.04$ and 0.08 bohr/fs, the DVV calculations are much more efficient than the GS−IRC method, with the latter requiring approximately 3 times as many Fock matrix evaluations and gradient evaluations. Figure 7 shows that the $\upsilon_0 = 0.08$ bohr/fs pathway lies slightly off of the GS−IRC and $\upsilon_0 = 0.04$ bohr/fs paths. Again, the time variation algorithm correctly detects this error and compensates by decreasing the time step and effectively slowing down the progress from the TS to the minima. Consequently, the number of Fock matrix evaluations actually increases from 2134 to 2518 when υ_0 is increased from 0.04 to 0.08 bohr/fs.

F. $[Ir(CO)_2I_3(CH_3)]^- \rightarrow [Ir(CO)I_3(COCH_3)]^-$. This reaction represents an important step in methanol carbonylation using an iridium based catalyst that has been the subject of a number of studies reported in the literature.[36−41] Recently, Cheong, Schmid, and Ziegler provided theoretical insight to the reaction pathway.[42] This system has been included to highlight the present method's efficiency for larger chemical systems. Calculations have been carried out at the HF/LanL2DZ level of theory with υ_0 set to 0.04 bohr/fs. Figure 8 shows the relationship between the C—C bond and potential energy. The DVV pathway agrees with the GS−IRC path very well. The DVV calculation requires 1078 Fock matrix evaluations, whereas the GS−IRC algorithm requires 9579 Fock matrix evaluations to map out the reaction path. The number of gradient evaluations also differs by a similar factor. The DVV method gains its efficiency over the GS−IRC model from two factors in this case. First, the DVV path is propagated much faster than the GS−IRC path. In fact, DVV takes an average step along the path of 0.154 au, whereas the GS−IRC takes an average step of 0.084 au. Second, DVV is an explicit method and does not require an optimization involving additional electronic structure calculations to correct each step. For this system, the GS−IRC algorithm requires an average of 3.253 gradient calculations per step, compared to 1 gradient calculation per step for DVV.

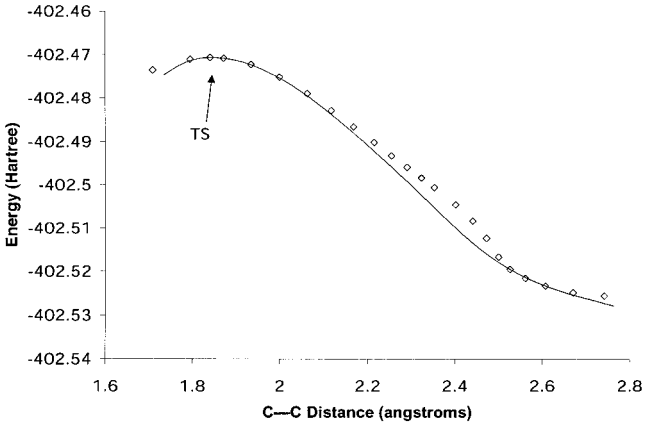

Figure 8. Reaction path following for $Ir(CO)_2I_3(CH_3)^- \rightarrow Ir(CO)I_3(COCH_3)^-$ [DVV path with υ_0 equal to 0.04 (◇) bohr/fs and GS−IRC path (solid line)].

IV. Conclusions

We have developed a damped classical trajectory algorithm for following reaction paths that closely approximate the IRC

paths. DVV pathways are very stable at conservative settings for v_0 (0.04 bohr/fs), and often follow the IRC path accurately with larger v_0 values. For small systems and high symmetry, the DVV method is not as efficient as the GS−IRC algorithm. However, for larger and more complex systems the DVV algorithm is much more efficient than the GS−IRC procedure with its default settings. Thus, the DVV reaction path following approach offers an efficient and stable alternative to the GS−IRC method that is especially attractive when studying larger systems.

Acknowledgment. We are grateful to Dr. J. M. Millam for helpful and insightful discussions throughout the duration of the project. H.P.H. thanks the Institute for Scientific Computing at Wayne State University for support provided by a NSF-IGERT Fellowship. This work was supported by a grant from the National Science Foundation (CHE 9874005).

References and Notes

(1) Bell, S.; Crighton, J. S. *J. Chem. Phys.* **1984**, *80*, 2464.
(2) Foresman, J. B.; Frisch, A. *Exploring Chemistry with Electronic Structure Methods*, 2nd ed.; Gaussian Inc.: Pittsburgh, PA, 1996.
(3) Head, J. D.; Zerner, M. C. *Adv. Quantum Chem.* **1989**, *20*, 239.
(4) McKee, M. L.; Page, M. *Rev. Comput. Chem.* **1993**, *4*, 35.
(5) Schlegel, H. B. *J. Comput. Chem.* **1982**, *3*, 214.
(6) Schlegel, H. B. *Adv. Chem. Phys.* **1987**, *67*, 249.
(7) Schlegel, H. B. In *Modern Electronic Structure Theory*; Yarkony, D. R., Ed.; World Scientific: Singapore, 1995.
(8) Thompson, L. In *Encyclopedia of Computational Chemistry*; Schleyer, P. v. R., Allinger, N. L., Clark, T., Gasteiger, J., Kollman, P. A. III., H. F. S., Schreiner, P. R., Eds.; Wiley: Chichester, 1998; p 3056.
(9) Fukui, K. *Acc. Chem. Res.* **1981**, *14*, 363.
(10) Schlegel, H. B. In *Encyclopedia of Computational Chemistry*; Schleyer, P. v. R., Allinger, N. L., Clark, T., Gasteiger, J., Kollman, P. A. III., H. F. S., Schreiner, P. R., Eds.; Wiley: Chichester, 1998; p 2432.
(11) Collins, M. A. *Adv. Chem. Phys.* **1996**, *93*, 389.
(12) Schmidt, M. W.; Gordon, M. S.; Dupuis, M. *J. Am. Chem. Soc.* **1985**, *107*, 2585.
(13) Ishida, K.; Morokuma, K.; Komornicki, A. *J. Chem. Phys.* **1977**, *66*, 2153.
(14) Baldridge, K. K.; Gordon, M. S.; Steckler, R.; Truhlar, D. G. *J. Phys. Chem.* **1989**, *93*, 5107.
(15) Garrett, B. C.; Redmon, M. J.; Steckler, R.; Truhlar, D. G.; Baldridge, K. K.; Bartol, D.; Schidt, M. W.; Gordon, M. S. *J. Phys. Chem.* **1988**, *92*, 1476.
(16) Page, M.; McIver, J. M. *J. Chem. Phys.* **1988**, *88*, 922.
(17) Page, M.; Doubleday, C.; McIver, J. W. *J. Chem. Phys.* **1990**, *93*, 5634.
(18) Sun, J. Q.; Ruedenberg, K. *J. Chem. Phys.* **1993**, *99*, 5269.
(19) Müller, K.; Brown, L. D. *Theor. Chim. Acta* **1979**, *53*, 75.
(20) Gonzalez, C.; Schlegel, H. B. *J. Chem. Phys.* **1989**, *90*, 2154.
(21) Gonzalez, C.; Schlegel, H. B. *J. Phys. Chem.* **1990**, *94*, 5523.
(22) Gonzalez, C.; Schlegel, H. B. *J. Chem. Phys.* **1991**, *95*, 5853.
(23) Gear, C. W. *Numerical Initial Value Problems in Ordinary Differential Equations*; Prentice Hall: Englewood Cliffs, 1971.
(24) Bunker, D. L. *Methods Comput. Phys.* **1971**, *10*, 287.
(25) Raff, L. M.; Thompson, D. L. In *Theory of Chemical Reaction Dynamics*; CRC: Boca Raton, 1985.
(26) *Advances in Chemical Trajectory Methods*; Hase, W. L., Ed.; JAI: Stamford, 1991; Vol. 1−3.
(27) Bolton, K.; Hase, W. L.; Peshlherbe, G. H. In *Modern Methods for Multidimensional Dynamics Computation in Chemistry*; Thompson, D. L., Ed.; World Scientific: Singapore, 1998; p 143.
(28) Gordon, M. S.; Chaban, G.; Taketsugu, T. *J. Phys. Chem.* **1996**, *100*, 11 512.
(29) Maluendes, S. A.; Dupuis, M. J. *J. Chem. Phys.* **1990**, *93*, 5902.
(30) Stewart, J. J. P.; Davis, L. P.; Burggraf, L. W. *J. Comput. Chem.* **1987**, *8*, 1117.
(31) Clementi, E.; Corongiu, G.; Lie, G. C.; Niesar, U.; Procacci, P. In *MOTECC: Modern Techniques in Computational Chemistry*; Clementi, E., Ed.; ESCOM: New York, 1989; Chapter 8.
(32) Frisch, M. J.; Trucks, G. W.; Schlegel, H. B.; Scuseria, G. E.; Robb, M. A.; Cheeseman, J. R.; Zakrzewski, V. G.; J. A. Montgomery, J.; Stratmann, R. E.; Burant, J. C.; Dapprich, S.; Millam, J. M.; Daniels, A. D.; Kudin, K. N.; Strain, M. C.; Farkas, O.; Tomasi, J.; Barone, V.; Mennucci, B.; Cossi, M.; Adamo, C.; Jaramillo, J.; Cammi, R.; Pomelli, C.; Ochterski, J.; Petersson, G. A.; Ayala, P. Y.; Morokuma, K.; Malick, D. K.; Rabuck, A. D.; Raghavachari, K.; Foresman, J. B.; Ortiz, J. V.; Cui, Q.; Baboul, A. G.; Clifford, S.; Cioslowski, J.; Stefanov, B. B.; Liu, G.; Liashenko, A.; Piskorz, P.; Komaromi, I.; Gomperts, R.; Martin, R. L.; Fox, D. J.; Keith, T.; Al-Laham, M. A.; Peng, C. Y.; Nanayakkara, A.; Challacombe, M.; Gill, P. M. W.; Johnson, B.; Chen, W.; Wong, M. W.; Andres, J. L.; Gonzalez, C.; Head-Gordon, M.; Replogle, E. S.; Pople, J. A. *Gaussian 99, Development Version (Revision C.02)*; Gaussian, Inc.: Pittsburgh, PA, 2000.
(33) Press, W. H. *Numerical Recipes in Fortran 77: The Art of Scientific Computing*, 2nd ed.; Cambridge University Press: Cambridge [England]: New York, 1996.
(34) Kato, S.; Morokuma, K. *J. Chem. Phys.* **1980**, *73*, 3900.
(35) Ayala, P. Y.; Schlegel, H. B. *J. Chem. Phys.* **1997**, *107*, 375.
(36) Ellis, P. R.; Pearson, J. M.; Haynes, A.; Adams, H.; Bailey, N. A.; Maitlis, P. M. *Organometallics* **1994**, *13*, 3215.
(37) Brodzki, D.; Denise, B.; Pannetier, G. *J. Mol. Catal.* **1977**, *2*, 149.
(38) Matsumoto, T.; Mizoroki, T.; Ozaki, A. *J. Catal.* **1978**, *51*, 96.
(39) Foster, D. *Adv. Organomet. Chem.* **1979**, *17*, 255.
(40) Foster, D. *J. Chem. Soc., Dalton Trans.* **1979**, *1979*, 1639.
(41) Dekleva, T. W.; D., F. *Adv. Catal.* **1986**, *34*, 81.
(42) Cheong, M.; Schmid, R.; Ziegler, T. *Organometallics* **2000**, *19*, 1973.